Tellus (1992), *44A*, 381–394

Simple formulation of turbulent mixing in the stable free atmosphere and nocturnal boundary layer

By JINWON KIM and L. MAHRT, *Department of Atmospheric Sciences, Oregon State University, Corvallis, OR 97331, USA*

(Manuscript received 5 April 1991; in final form 15 May 1992)

ABSTRACT

Turbulent mixing lengths and the eddy Prandtl number are estimated by analyzing aircraft data from three different field programs and existing studies in the literature. For small scale turbulence, the estimated mixing lengths appear to decrease rapidly with increasing Richardson number (Ri) and then reach an approximately constant value of 2.5 m for Ri > 0.3 with large scatter. A least squares fit of the estimated mixing length for heat using the format of Louis et al. (1981) yields an asymptotic mixing length of 14.2 m for neutral stratification. This value represents the best fit to the turbulent fluxes for the observed cases of stratified flow rather than a direct calibration of turbulence in neutrally stratified flow for which there were no observations. Mixing length values estimated from stronger larger scale disturbances also show a decrease of mixing length with increasing Richardson number although the values of mixing lengths are categorically larger yielding an asymptotic value of 150 m. Apparently, the Richardson number by itself is not a good predictor for the strength of turbulent mixing although suitable alternatives for large scale models are not available. The Prandtl number increases with increasing Richardson number in agreement with previous studies but the scatter is large. The mixing length formulation is applied to a column model of the lower troposphere. The asymptotic mixing length and the stability-dependent Prandtl number are derived from the data analysis. For the very stable case, shear generation of turbulence in the upper part of the surface inversion layer can be more significant than surface based turbulence generation. Large scale subsidence may significantly reduce the depth of the overlying residual layer. Since the subsidence is difficult to estimate from observations, model comparisons with the observed data are not conclusive.

1. Introduction

The mixing and dissipation of large scale kinetic energy by clear air turbulence in the free atmosphere plays an important role in the long term evolution and energetics of atmospheric motions. Previous studies suggest that as much as 25% of the dissipation of atmospheric kinetic energy occurs through clear air turbulence in the mid- and upper-troposphere (Heck et al., 1977). The modeling studies of Louis et al. (1981) show that the features of simulated synoptic and global scale flows are sensitive to the parameterization of turbulent mixing. Despite this importance, turbulent mixing in the free atmosphere has received much less attention in comparison to the surface-based boundary layer partly due to the lack of observations.

Turbulence in the free atmosphere is thought to occur in regions of small Richardson number. Early studies of such a relationship are summarized in Vinnichenko et al. (1973). Strong clear air turbulence is observed near the jet stream and internal fronts (Kennedy and Shapiro, 1975). Clear air turbulence is also induced by smaller scale atmospheric perturbations such as breaking gravity waves (Atlas et al., 1970).

Turbulent mixing sometimes occurs systematically in the residual layer, a weakly stratified remnant of the daytime mixed layer remaining above the nocturnal boundary layer (Stull, 1990). Observational (Lenschow et al., 1987) and numerical studies (André et al., 1978; Garratt, 1985; Stull and Driedonks, 1987) indicate the occurrence of shear-driven turbulence at the top and/or bottom of the residual layer. Intermittent turbulence can develop in the upper part of the nocturnal surface inversion layer and bottom of the residual layer due to local shear not directly related to the surface stress (Mahrt, 1985a). Such turbulence may propagate downward in the form of turbulent bursts (Nappo, 1991). Consequently, models based on boundary-layer similarity appear to poorly describe the very stable case.

Previous simple parameterizations of mixing in the free atmosphere are generally posed in terms of the Richardson number. For example, Keller (1990) chooses a critical Richardson number of unity for the onset of clear air turbulence. Laboratory experiments and oceanic observations generally support the gradient Richardson number criterion for the onset of turbulence (e.g., Thorpe, 1973; Fernando, 1991). However, the perceived critical value of the Richardson number may increase with the depth of the layer over which it is computed (Lyons et al., 1964). Even with large values of the Richardson number for the resolved flow, the Richardson number on smaller scales may become sufficiently small to initiate local turbulence (Padman and Jones, 1985). The observational study of Kunkel and Walters (1982) inferred turbulence at Richardson number values as large as 10. In the laboratory measurements of DeSilva and Fernando (1992), the Richardson number by itself is unable to predict the mixing characteristics. The role of the Richardson number in clear air turbulence might be further complicated by the possibility that destruction of turbulence by buoyancy occurs at scales smaller than the principal scale of shear generation of turbulence (Dutton, 1969). In a bora flow, Mahrt (1985b) found only modest correlation between spatial variations of the turbulence and the local Richardson number partly due to spatial inhomogeneity and advection of turbulence.

Some formulations of turbulent mixing in the atmosphere above the boundary layer employ an asymptotic mixing length and a dependence on the Richardson number adopted from surface layer similarity theory (Blackadar, 1962; Louis, 1979; Louis et al., 1981). Even though such formulations have been used in the numerical simulation of larger scale flow, the validity of this similarity theory in the free atmosphere is yet to be examined directly from observations of turbulence. Ueda et al. (1981) observed that the relationship between the eddy diffusivities and the Richardson number is quite different in the surface layer compared to that above the surface layer. Therefore in this study, we will estimate turbulent fluxes and their relation to the Richardson number by analyzing aircraft data above the boundary layer taken during three different field programs (Section 2). In addition, turbulent mixing lengths and eddy Prandtl numbers are estimated from fluxes presented in Mahrt (1985a), Lenschow et al. (1987), and Kennedy and Shapiro (1980). Based on analyses of these data, we attempt to evaluate the mixing length formulation by Louis et al. (1981) for application to the stably stratified atmosphere (Sections 3–4). Our analysis focuses on whether the observed mixing length depends systematically on the Richardson number. In Section 5, the influence of turbulent mixing on the evolution of low level flow is studied using a column model with emphasis on the residual layer above the nocturnal boundary layer.

2. Data

On 5 May 1983 in CABLE (Clear Air Turbulence and Boundary Layer Experiment), the King Air from the National Center for Atmospheric Research flew from 0600 to 1000 LST in the east-west direction over western Kansas, USA (Fig. 1a). Layers of turbulence occurred above the thin but growing boundary layer. Flights on 24 May 1983 in CABLE extended from Oklahoma City to over the Gulf of Mexico during the period from 1600 to 1900 LST. On this day, clear air turbulence occurs approximately 3 km above the sea surface (Fig. 1b). Based on the isentropic analysis (Fig. 1b), this turbulence apparently occurs in conjunction with mesoscale disturbances. Data on 6 May 1979 in SESAME (Severe Environmental Storms and Mesoscale Experiment) were taken in and above a windy, weakly stable nocturnal boundary layer over central Oklahoma, USA (Lenschow et al., 1987). Fluxes are also used from the International Cirrus Experiment (ICE) as computed by Quante (1989).

After high-pass filtering the aircraft data to partially remove gravity waves and other larger scale

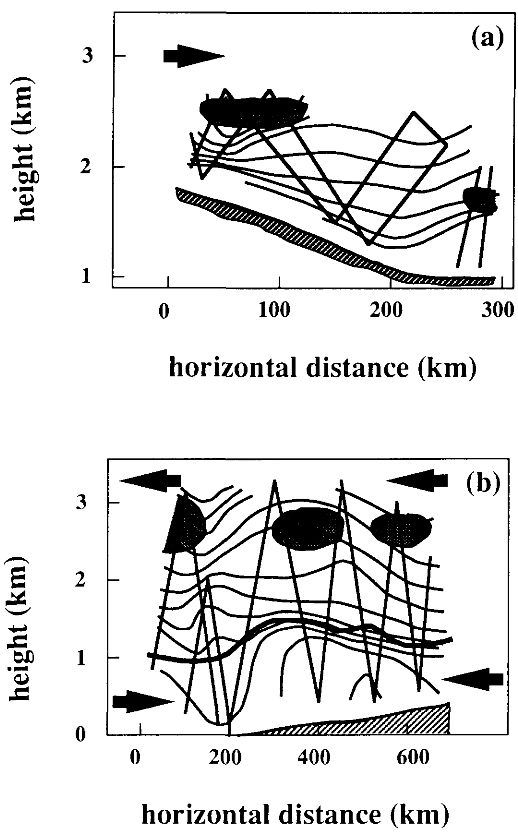

Fig. 1. Cross-section of CABLE observational regions for (a) 5 May 1983 and (b) 24 May 1983 for clear air turbulence (shaded); isentropes in 1°C intervals (solid lines), PBL top (thick solid line in b); aircraft flight paths (slant solid lines); and direction of the mean flow (thick arrows). Height is with respect to sea level.

disturbances, heat and momentum fluxes and the vertical velocity variances are calculated. Based on cospectra, the cutoff wavelength for the high-pass filtering is chosen to be 1 km for 5 and 24 May CABLE and 6 May SESAME. Examples of vertical profiles of potential temperature and variance of high-pass filtered vertical velocity for slant aircraft soundings from CABLE 24 May over the ocean are presented in Fig. 2. The observed clear air turbulence is separated from boundary-layer turbulence by a layer of relatively small vertical velocity variance (Fig. 2). The bottom of the near-quiescent layer coincides with the capping inversion at the top of the boundary layer as can be seen from the potential temperature profile (Fig. 2).

Elevated maxima of downward turbulent heat flux also appear in the same layers as the vertical velocity variance maxima. The variance of the high-pass filtered vertical velocity in the patches of clear air turbulence corresponds to a root-mean-square vertical velocity of 10–60 cm s^{-1} for the CABLE cases, 5–40 cm s^{-1} for SESAME 6 May, and about 10 cm s^{-1} for ICE. The vertical velocity of the stronger updrafts and downdrafts are usually an order of magnitude larger than the root-mean-square vertical velocity.

The vertical profiles of the mean flow in CABLE and SESAME are estimated from slant soundings by block averaging the raw data. The depth of the averaging interval is typically 50 m. It is specified for each leg based on subjective assessment of natural layering, the aircraft ascent or descent rate, and the need to reduce the contamination by horizontal variability due to mesoscale motions. To obtain the mean values at the levels corresponding to the top and bottom of the turbulent layer, the averaged variables are interpolated with cubic splines. For the ICE data, the mean flow profiles are obtained by horizontal averaging along the flight path at each flight level.

For SESAME and CABLE, the gradient Richardson numbers calculated for the turbulent layers vary from 0.2 to 1.0 even though the turbulence appears to be fully developed. The calculation of the gradient Richardson number included any jump in properties at the lower and upper edges of the turbulent layer where entrainment appears to occur. Gradients within the turbulent layer may become vanishingly small. Values of the Richardson number calculated across layers away from the turbulent layers are usually larger than 1.5 although in a few exceptions the gradient Richardson number is as small as 0.6. When the block-averaging intervals were increased by a factor of two without changing the total depth over which the Richardson number is computed, the resulting gradient Richardson numbers changed by an average amount of approximately 50% with no preference for the sign of the changes.

For ICE, the smallest vertical interval is fixed by the levels of the horizontal aircraft flights. Computing the Richardson number between non-adjacent flight levels indicates that for this data the Richardson number generally increases with the thickness of the layer over which the Richardson number is calculated.

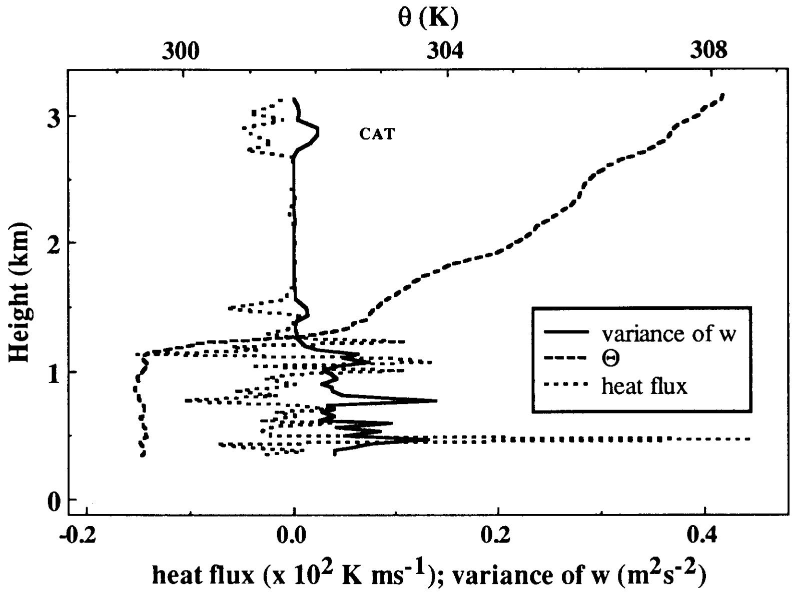

Fig. 2. Vertical profiles of variance of high-pass filtered vertical velocity (solid line), heat flux × 100 (short dashed line), and potential temperature (long dashed line) observed on 24 May CABLE.

3. Eddy diffusivity

In this section, we construct an empirical formulation for the eddy diffusivity in the free atmosphere in terms of the large scale stability based on the gradient Richardson number. The gradient Richardson number is approximated by the *layer Richardson number* (R_L) computed across the bulk turbulent layer as

$$R_L = \frac{g}{\Theta} \frac{\Delta\Theta \, \Delta z}{|\Delta V|^2}, \tag{1}$$

where g is the gravitational acceleration, $\Delta\Theta$ is the difference of the mean potential temperature across the turbulent layer of the thickness Δz, Θ is the mean potential temperature of the layer, and ΔV is the magnitude of the wind vector difference across the layer. We express the eddy diffusivity for heat (K_h) and momentum (K_m) in terms of the turbulent mixing length (l_h) and the eddy Prandtl number (Pr) as

$$K_h = l_h^2 \left| \frac{\partial V}{\partial z} \right|, \tag{2}$$

$$K_m = K_h \mathrm{Pr}. \tag{3}$$

The turbulent mixing length for heat and the eddy Prandtl number will be assumed to depend on the Richardson number. These dependencies on the Richardson number will be estimated from the observations. Mixing lengths computed from the momentum flux showed considerably more scatter than those estimated from the heat flux. Horizontal velocity fluctuations and associated momentum flux are influenced by pressure fluctuations whereas temperature fluctuations are not. Mahrt and Gibson (1992) found that the estimation of the momentum flux requires significantly longer record lengths compared to that needed for the heat flux. We first establish the formulation of the eddy diffusivity for heat and then estimate the eddy diffusivity for momentum from the dependence of the eddy Prandtl number on the Richardson number.

We compute eddy diffusivities from the observed turbulent fluxes and vertical variation of the mean flow as

$$K_h = -\frac{\overline{w'\theta'}}{\partial\Theta/\partial z}, \tag{4a}$$

$$K_m = -\frac{\overline{u'w'}(\partial U/\partial z) + \overline{v'w'}(\partial V/\partial z)}{(\partial U/\partial z)^2 + (\partial V/\partial z)^2}, \tag{4b}$$

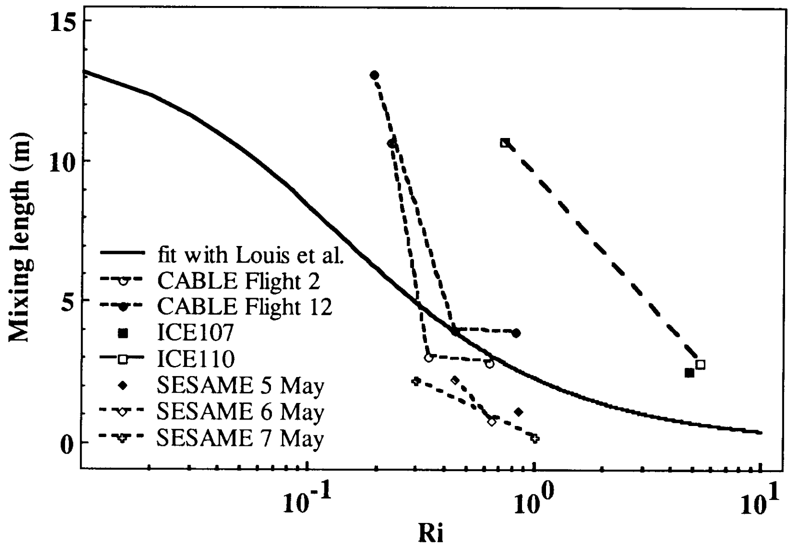

Fig. 3. Mixing lengths from CABLE, SESAME, and ICE and the nonlinear least-squares fit with Louis et al. (1981) model (7). Data from each flight is averaged over the intervals of the Richardson number: $\mathrm{Ri} \leqslant 0.25$, $0.25 < \mathrm{Ri} \leqslant 0.5$, $0.5 < \mathrm{Ri} \leqslant 1$, and $\mathrm{Ri} > 1$.

where primed variables denote the high-pass filtered variables and the overbar designates an average along the flight path.

The mixing length can be obtained from the eddy diffusivity for heat (2) as

$$l_{\mathrm{h}}^2 = \frac{K_{\mathrm{h}}}{|\partial V / \partial z|}. \tag{5}$$

The mixing lengths computed from the CABLE, SESAME, and ICE data are nearly independent of the Richardson number for values greater than about 0.3. For this regime the average value of the mixing length is only about 2.5 m although the scatter is large (Fig. 3). The scatter is probably due to the difficulty of estimating weak fluxes and due to nonstationary interplay between the evolving turbulence and adjusting mean flow profiles. In spite of small values of the mixing length, the flow appears to be fully turbulent in the regions where fluxes are computed. The small mixing length values may be related to the small vertical extent of turbulence. The two cases for the Richardson number less than 0.25 show the expected increase of the mixing length with decreasing stability.

The mixing length for heat is also computed from Kennedy and Shapiro (1980) observed near an upper tropospheric front (Fig. 4). For this case the mixing lengths are an order of magnitude larger, perhaps reflecting the transport by vigorous eddies and large scale disturbances on horizontal scales up to tens of kilometers. Comparing Figs. 3 and 4 verifies that the mixing length, for a fixed Richardson number, is larger for larger scale turbulence.

The large scatter of the data (Fig. 3) does not permit refinement of the dependence of the mixing

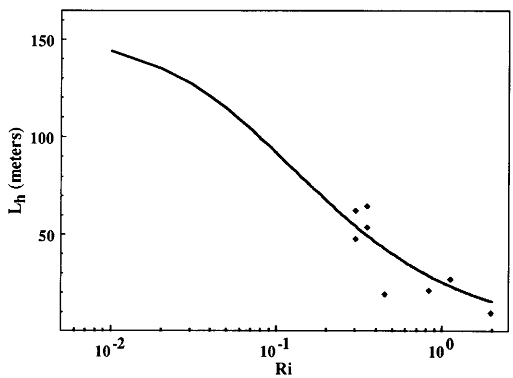

Fig. 4. Mixing lengths from Kennedy and Shapiro (1980) and the least squares fit with the Louis et al. (1981) model (7).

length on the Richardson number. We will therefore calibrate the mixing length formulation of Louis et al. (1981) by adjusting the asymptotic mixing length at neutral stratification to best fit the data from CABLE, SESAME, and ICE for values of the Richardson number within the range between 0 and 1. In the formulation of Louis et al. (1981), the mixing length for heat can be related to the Richardson number by means of a nondimensional function ϕ_h and the asymptotic value of the mixing length $l_{0,h}$ for vanishing stratification. Then we may write

$$l_h(\mathrm{Ri}) = l_{0,h}\phi_h(\mathrm{Ri}). \qquad (6)$$

With application to numerical models, the Richardson number is computed over each grid interval. The actual turbulence can occur over thinner layers and may be intermittent. The latter may collectively lead to diffusion across a thicker layer corresponding to vertical grid interval. Therefore turbulent diffusion can occur even when the Richardson number over the grid interval is large. For this reason, formulations of clear air turbulent transport for large scale models might adopt a smooth dependence on the Richardson number as in the formulation of Louis et al. (1981), even though the local transport might be governed by a critical Richardson number.

In the formulation of Louis et al. (1981), $\phi_h(\mathrm{Ri})$ for a stably stratified atmosphere is given as

$$\phi_h(\mathrm{Ri}) = [1 + 15\mathrm{Ri}(1 + 5\mathrm{Ri})^{1/2}]^{-1/2}. \qquad (7)$$

A least squares fit of the mixing lengths estimated from CABLE, SESAME, and ICE yields an asymptotic mixing length of 14.2 m although the fit to the data is mediocre. This value of the asymptotic mixing length agrees with the study of Beljaars and Holtslag (1991). Following Wu (1965), Busack and Brümmer (1988) also found good prediction with a relatively small asymptotic value of 12.5 m for above the boundary layer. They used the mixing length formulation of Blackadar (1962) with the stability dependence adopted from Louis (1979).

These values of the mixing length are an order of magnitude smaller than those used in previous turbulent mixing formulations (Louis et al., 1981; NMC 1988). Such large model values appear to be in better agreement with the observations of Kennedy and Shapiro (1980) for strong turbulence near an upper level front. The asymptotic mixing length obtained by fitting the Louis et al. (1981) formulation to their data is approximately 150 m (Fig. 4). Transport by disturbances on horizontal scales as large as a few tens of kilometers seem to differentiate the Kennedy and Shapiro (1980) case from the other data sets. How can a numerical model make such a distinction? There appears to be no physical way to estimate the neutral asymptotic mixing length or the depth of turbulent layer. Free layers of atmospheric turbulence in neutrally stratified layers grow through vertical entrainment until stratification becomes a limiting factor; however equilibrium may not be achieved with normal atmospheric conditions. One approach for mutual adjustment of the Richardson number and turbulence can be found in Roach (1970). For the present study, the mixing length at neutral stability is actually an adjusted parameter providing the best fit over the observed range of the Richardson numbers rather than a direct representation of the neutral case.

Although Figs. 3, 4 suggest that the mixing length for very stable conditions decreases more slowly with the Richardson number than predicted by the Louis formulation, Figs. 3, 4 do not account for the increasing number of cases of nonturbulent flow with increasing Richardson number. This trend is observed both with the present data and the numerous studies summarized in Vinnichenko et al. (1973). Therefore modification of the relationship by Louis et al. (1981) does not seem justified without more extensive data.

4. The eddy Prandtl number

The eddy Prandtl number is estimated from the observed eddy diffusivities. The Prandtl number tends to increase with the Richardson number (Fig. 5) although the scatter is large, especially at Richardson numbers greater than 0.4. The increase of the Prandtl number to values greater than unity implies that the contribution of the pressure fluctuations to the vertical transport of horizontal momentum becomes more important as the stability of the mean flow increases. Increasing Prandtl number with increasing Richardson number has been observed in the laboratory experiments of Mizushina et al. (1978), Webster

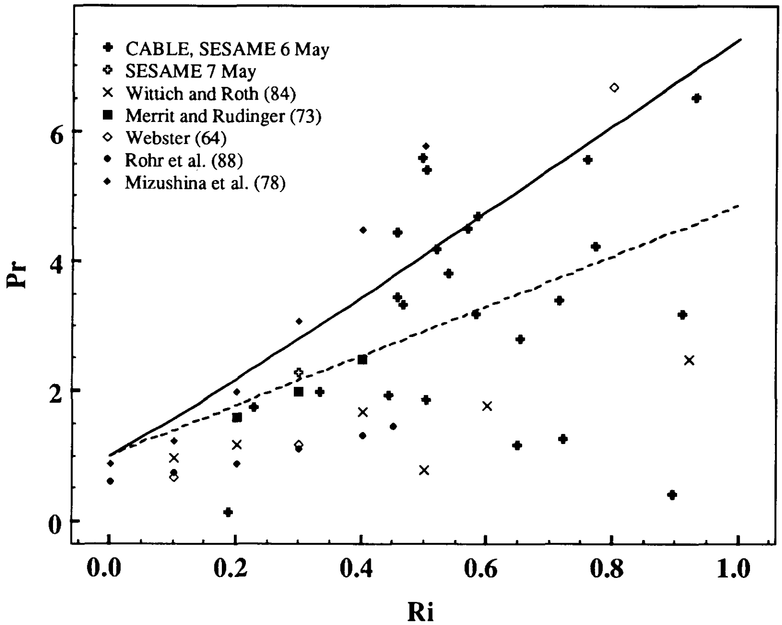

Fig. 5. Eddy Prandtl numbers from CABLE and SESAME. The dashed line is the least squares fit (8) and the solid line is the relationship derived from Louis et al. model (12) with $\mathrm{Pr}_0 = 1$.

(1964), Rohr et al. (1988), and in the atmospheric observations of Merrit and Rudinger (1973) and Wittich and Roth (1984), all plotted in Fig. 5.

The eddy Prandtl numbers estimated from the CABLE and SESAME data are approximated with a least-squares linear fit to the gradient Richardson number (solid line, Fig. 5) by forcing the Prandtl number to approach unity with vanishing Richardson number. Then

$$\mathrm{Pr(Ri)} = 1.0 + 3.8\mathrm{Ri}. \tag{8}$$

The eddy Prandtl number for the Louis model is obtained from (2), (3), and (6) as

$$\mathrm{Pr(Ri)} = \frac{l_\mathrm{m}^2}{l_\mathrm{h}^2}(\mathrm{Ri}) = \frac{l_{0,\mathrm{m}}^2}{l_{0,\mathrm{h}}^2}\frac{\phi_\mathrm{m}^2(\mathrm{Ri})}{\phi_\mathrm{h}^2(\mathrm{Ri})}, \tag{9}$$

where l_m, $l_{0,\mathrm{m}}$, and ϕ_m are the mixing length, the asymptotic mixing length, and the nondimensional function of the gradient Richardson number for the turbulent momentum flux, respectively. Defining a new dimensionless function of the gradient Richardson number $F(\mathrm{Ri})$, (9) becomes

$$\mathrm{Pr(Ri)} = \mathrm{Pr}_0 F(\mathrm{Ri}), \tag{10}$$

where Pr_0 is the eddy Prandtl number at neutral stability ($\mathrm{Ri} = 0$) and is expressed as

$$\mathrm{Pr}_0 = \frac{l_{0,\mathrm{m}}^2}{l_{0,\mathrm{h}}^2}. \tag{11}$$

The nondimensional function $F(\mathrm{Ri})$ is obtained from $\phi_\mathrm{h}(\mathrm{Ri})$ and $\phi_\mathrm{m}(\mathrm{Ri})$ given in Louis et al. (1981) as

$$F(\mathrm{Ri}) \equiv \frac{\phi_\mathrm{m}^2(\mathrm{Ri})}{\phi_\mathrm{h}^2(\mathrm{Ri})} = \frac{1 + 15\mathrm{Ri}(1+5\mathrm{Ri})^{1/2}}{1 + 10\mathrm{Ri}(1+5\mathrm{Ri})^{-1/2}}. \tag{12}$$

Based on the sensitivity tests with large scale models, Louis et al. (1981) suggest asymptotic mixing lengths of 150 and 450 m for the momentum and heat transfer, respectively. These values correspond to $\mathrm{Pr}_0 = \frac{1}{9}$, a value which is much smaller than implied from the observations. Relationship (12) also predicts that the Prandtl number increases with the Richardson number at a rate which is approximately linear and a little faster than predicted by the empirical formulation (8) (Fig. 5). The Prandtl number for the stronger turbulence observed by Kennedy and Shapiro

(1980) can be approximated by a slower increase with Richardson number

$$\mathrm{Pr(Ri)} = 1 + 2.1\mathrm{Ri}.$$

Formulation (8) is applied in the modeling study of the next section where only modest turbulence is expected.

5. Column model simulations

The influence of clear air turbulence above the nocturnal boundary layer is now investigated using a one-dimensional numerical model with the eddy diffusivity formulation (2–3) based on the stability dependent mixing length (6–7) and Prandtl number (8). Turbulent mixing in the boundary layer is calculated from the model of Troen and Mahrt (1986) except for special modifications developed in Subsection 5.3. Additional features of the column model are detailed in Ek and Mahrt (1990). This model is designed for use within large scale models where simplicity and economy are required.

To eliminate spurious inertial oscillation in the free atmosphere, the initial wind profiles are specified to be geostrophic above 200 m and decrease linearly with height below 200 m to zero at the surface. In the numerical simulations in Subsections 5.1–5.3, the mean vertical motion is specified to be zero, and the geostrophic winds are assumed to be time- and height-independent with a value of 5 ms^{-1}.

5.1. Diurnal variation

The model simulation is governed by the growth and decay of the mixed layer and attendant inertial oscillation. As a result, the nocturnal lower atmosphere evolves into three distinctive layers consisting of the nocturnal boundary layer, the residual layer, and the overlying free atmosphere (Fig. 7a). These layers also occur in more complicated form in the observations of Lenschow et al. (1987) plotted in Fig. 6.

The daytime mixed layer begins to collapse at 1700 solartime and yields to a nocturnal boundary layer of a few hundred meters depth. A residual layer of weak or vanishing stratification layer remains between the top of the nocturnal surface inversion layer and the overlying inversion corre-

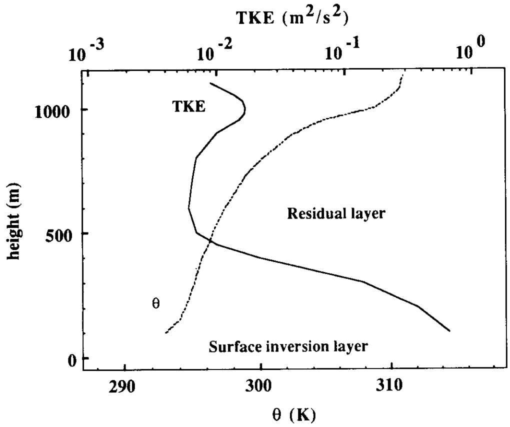

Fig. 6. Profiles of θ (dashed line) and turbulence kinetic energy (solid line) observed at 0640 on 7 May in SESAME (after Lenschow et al., 1987).

sponding to the top of the pre-existing daytime mixed layer. Modelling studies of André et al. (1978), Garratt and Brost (1981), Garratt (1985), and Stull and Driedonks (1987) also show the survival of the residual layer during the nighttime. The weakly stratified layer observed above the surface inversion layer in the early morning of 7 May in SESAME (Fig. 6) and observed in André et al. (1978), Mahrt et al. (1979), Hsu (1979), Estournel et al. (1986), and Stull and Driedonks (1987) may be examples of the residual layer. Following the mixed layer collapse and development of the low-level jet (Buajitti and Blackadar, 1957; Beyrich and Klose, 1988), significant vertical shear of the mean flow develops both at the top and bottom of the residual layer (Fig. 7b).

In actual atmospheric flows where the geostrophic wind varies spatially, horizontal convergence induced by inertial oscillations leads to damping by pressure adjustments (Smith and Mahrt, 1981) and presumably limits the magnitude of the low-level jet. These effects and large scale horizontal advection cannot be included in a column model.

5.2. Turbulence in the residual layer

By the early morning, when the modeled low-level jet reaches its full strength, the eddy diffusivity reaches a maximum in the shear layer on the upper side of the low-level jet (Fig. 7a, solid line) and reaches a weaker maximum near the top of the residual layer (not shown). A local turbulence maximum near the top of the residual

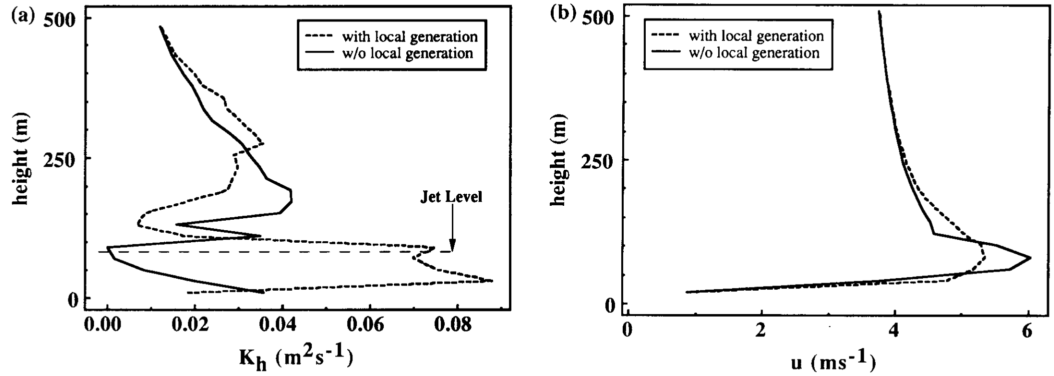

Fig. 7. Model-estimated vertical profiles at 0500 LST for (a) K_h and (b) u with $U_g = 5\ \mathrm{ms}^{-1}$ with (dashed lines) and without (solid lines) local generation of turbulence in the upper part of the surface inversion layer.

layer also occurs in the early morning profile of the turbulence kinetic energy on 7 May 1979 SESAME (Fig. 6), and in the model results of André et al. (1978) and Garratt (1985). An inferred maximum of turbulence near the low-level jet has been observed by André and Mahrt (1982) and is reported in the modeling studies of André et al. (1978) and Garratt (1985).

The modelled clear air turbulence reduces the mean shear near the top of the residual layer but is otherwise unimportant for this flow case. The potential temperature in the residual layer remains well mixed throughout the night and momentum remains partially mixed. As a result, the Richardson number and eddy diffusivity are sensitive to slight changes of the mean profiles and can even be altered by changes in the time step; however, the resulting turbulent fluxes are categorically small for these cases and have little effect on the mean flow.

Fig. 6 and previous observations indicate that the residual layer often develops some stratification during the night even if weak. The failure of the model to develop such stratification may be due to underestimation of mixing at the top and bottom of the residual layer or due to neglect of clear air radiative cooling, horizontal advection, baroclinity (Subsection 5.4), and mean subsidence (Subsection 5.5). Significant clear air radiative cooling was inferred from observations for the lower part of the residual layer in André and Mahrt (1982) and occurred in the modelling study of Garratt and Brost (1981). Application of a larger asymptotic mixing length of 150 m deduced from Kennedy and Shapiro (1980) significantly reduces the modeled shear near the top of the residual layer, but still fails to stratify the interior of the residual layer.

Even larger asymptotic mixing lengths are specified for large scale numerical models (Louis et al., 1981; NMC 1988) which produce an order of magnitude larger eddy diffusivity than that estimated from the present observations. These model mixing lengths are based on model performance rather than on observations and may attempt to include subgrid variability of turbulence (Maryon, 1990). The present analysis of observations supporting the asymptotic mixing length of 14.2 m includes fluxes on horizontal scales up to 1 km only and does not explicitly include gravity-wave-induced turbulence nor direct transport of momentum by gravity waves.

5.3. *Turbulence in the upper part of the nocturnal boundary layer*

Although models based on boundary-layer similarity theory appear to adequately approximate the weakly stratified boundary layer, they poorly describe the strongly stratified boundary layer. Boundary-layer similarity theory is based on the assumption that the vertical length scale of the mixing is related to the depth of the boundary layer and height above the ground. In the very stable boundary layer, vertical movement of air is restricted by buoyancy and the turbulent eddies cannot extend over the entire depth of the boundary layer (Nieuwstadt, 1984) sometimes leading to only intermittent turbulence even close

Tellus A/44/5-3

to the surface (Kondo et al., 1978). For example, the formulation for the stable boundary layer employed in the present model fails to represent the effect of significant shear in the upper part of the nocturnal surface inversion layer associated with the overlying low-level jet. The observed nocturnal boundary layer may assume an upside down structure with the main source of shear generation occurring near the top of the surface inversion layer (Mahrt, 1985a).

The local scaling model of Nieuwstadt (1984) provides more flexibility but requires the flux to vanish at the top of the boundary layer and cannot include the case where shear at the top of the surface inversion layer is a principal source of turbulence. We will attempt to include local generation of turbulence in the upper part of the nocturnal boundary layer by merging the present free atmospheric mixing model with the modeled nocturnal boundary layer. It is arbitrarily assumed that boundary-layer similarity is always valid below $0.3h$, the level of maximum eddy diffusivity in the similarity model, where h is the boundary-layer depth. The merged model allows local shear generation of mixing to override the conventional boundary-layer prediction above $0.3h$ if the local prediction of the eddy diffusivity (2, 6–7) is greater than the boundary-layer prediction. The asymptotic mixing length $l_{0,\mathrm{h}}$ in (5) is not allowed to exceed kz for the local eddy diffusivity formulation where k is the von Kármán constant, assumed to be 0.4, and z is the height above the surface. That is, *free* eddies in the stable boundary layer attempting to become larger than kz would become constrained by the surface. Unfortunately, there are no turbulence observations to study the development of turbulence from elevated shear layers which subsequently become influenced by the ground.

The eddy diffusivity estimated by the local prediction significantly exceeds the eddy diffusivity estimated from the boundary-layer similarity theory late in the night when shear near the top of the surface inversion layer becomes significant (Fig. 7a, broken line). As a result, the maximum eddy diffusivity in the early morning occurs in the upper part of the nocturnal boundary layer on the underside of the low level wind maxima (Fig. 7a) as is also inferred from the observations of André and Mahrt (1982) and Mahrt et al. (1979). An elevated local maximum of the eddy diffusivity was observed in the nocturnal boundary layer analysis of Yasuda (1988). For the present numerical experiment, the locally generated turbulence reduces the low-level wind speed maximum by 10% but otherwise exerts negligible influence on the mean flow (Fig. 7b). However as the specified geostrophic wind speed decreases, the relative influence of local turbulence generation increases. That is, the modeled local generation of turbulence in the stable boundary becomes *relatively* more important when turbulence in the boundary layer is weak.

The 20 m temperature is about 2°C warmer when local mixing is included in the upper part of the nocturnal boundary layer. Overestimation of surface cooling has been a systematic deficiency of boundary-layer models applied to very stable conditions (Ruscher, 1987). Consequently, the modeled downward heat flux into the stable boundary layer by inclusion of local shear generation may allow removal of artificial constraints in low resolution large scale models. Such constraints include specification of a minimum low-level wind speed (NMC 1988) and limitation of the influence of stratification on the surface exchange coefficient (M. Schlesinger and T. Scholtz, personal communications).

5.4. *Baroclinity*

Mean shear and generation of turbulent mixing in the residual layer may be enhanced by baroclinity of the large scale flow. We study the influence of geostrophic wind shear on the generation of turbulence by arbitrarily specifying the geostrophic wind to increase linearly from 4 ms^{-1} at the ground to 8 ms^{-1} at 2 km above the ground. Horizontal advection of temperature implied by the geostrophic wind shear is neglected.

With the imposed geostrophic wind shear, local generation of turbulence in the upper part of the nocturnal boundary layer smooths the potential temperature profile and reduces the speed of the nocturnal jet by as much as 20% (Fig. 8). The 20 m temperature becomes about 4°C warmer when local mixing is included in the upper part of the nocturnal boundary layer (Fig. 8b). However, the enhanced mixing due to baroclinity still fails to stratify the residual layer. Unfortunately, our observations do not allow adequate estimation of the geostrophic wind shear to test the column model.

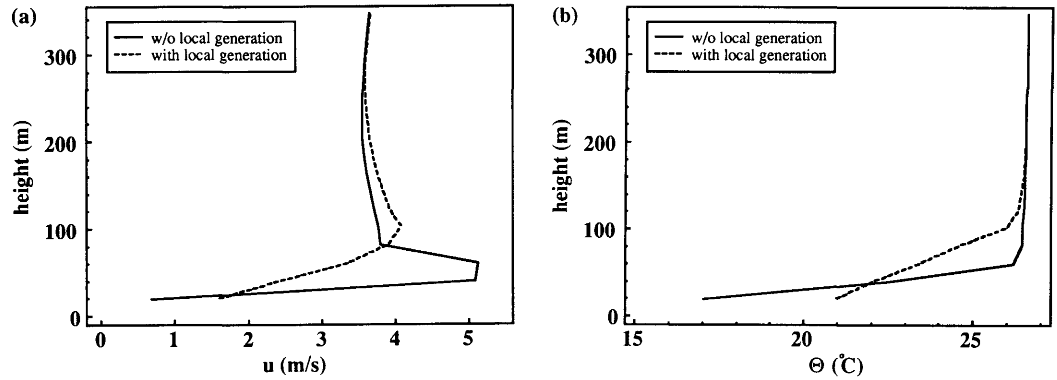

Fig. 8. Vertical profiles at 0500 LST for nonzero geostrophic wind shear for (a) u and (b) θ simulated with (dashed lines) and without (solid lines) local generation of turbulence in the upper part of the surface inversion layer.

5.5. Large-scale subsidence

Since the residual layer does not grow significantly by entrainment, large scale subsidence $W(z)$ will reduce the thickness of the residual layer during a period τ by roughly $W(z)\tau$. As an arbitrary example, the influence of large scale subsidence is studied by specifying the mean vertical velocity profile to be $-2.5\ \mathrm{cms}^{-1}$ at 3 km and to decrease linearly to zero at the ground. The numerical simulation is otherwise identical to that of Subsection 5.1.

The vertical advection of potential temperature due to subsidence together with weak mixing generate weak stratification in the upper part of the residual layer (Fig. 9b). The subsidence reduces the thickness of the residual layer to less than half of that without subsidence (Fig. 9). These results suggest that realistic values of the subsidence may be quite important. However, a major difficulty for comparing the modeled residual layer with observations now emerges. The depth of the residual layer is sensitive to even modest values of subsidence; yet, subsidence cannot be accurately estimated from observations. For example, an error of 1 cm^{-1} over a period 9 hours changes the thickness of the residual layer by more than 300 m.

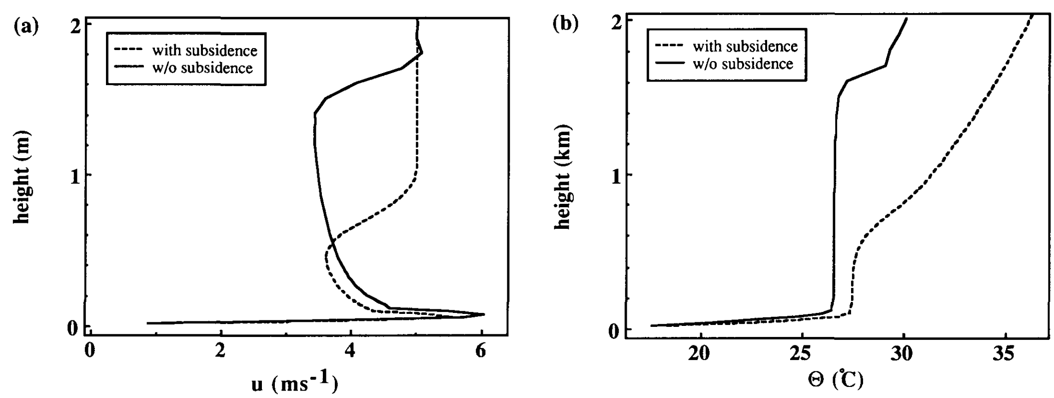

Fig. 9. Vertical profiles of (a) u and (b) θ with (dashed line) and without (solid line) subsidence.

6. Conclusions

Clear air turbulent fluxes have been estimated from aircraft data obtained during the SESAME, CABLE, and ICE programs and from Kennedy and Shapiro (1980) in order to evaluate the relationship between the mixing length and the Richardson number. The observed mixing length tends to show the expected decrease with the Richardson number, at least for small values of the Richardson number. The observed values of the mixing length are generally smaller than those employed by existing formulations. However, the scatter is large and large systematic differences occur between the different data sets. Within the large scatter of the data, the formulation of Louis et al. (1981) with recalibrated asymptotic mixing length seems adequate throughout the troposphere above the boundary layer including the upper part of the nocturnal surface inversion layer. The large scatter of data does not permit adjustment of the stability function.

Measurements of turbulent fluxes and their relationship to the Richardson number could be affected by significant sampling problems. Other problems are sensitivity to the depth of the layer over which the Richardson number is computed, nonstationarity due to generation and collapse of the turbulence, and modification of the Richardson number by the turbulence. Influences on the turbulence not included in the Richardson number may also be important. For example, the above data analysis suggests that the mixing length increases with the horizontal scale contributing to the flux. As a result, the mixing length inferred from Kennedy and Shapiro (1980) is an order of magnitude larger than those from the three other field programs. Partly because of the above complications, any relationship between the turbulence and Richardson number is characterized by large scatter. The value of the Richardson number may indicate the probability of initiation of turbulence better than predict the flux due to established turbulence. The data analysis also suggests that the current use of large mixing lengths in large scale models can not be justified from existing observations of clear air turbulence. Larger mixing lengths might help represent fluxes by disturbances larger than turbulent scales although there is no evidence that such transport is governed by a Richardson number dependence.

The formulation of mixing length for heat constructed by Louis et al. (1981) has been calibrated to the above turbulence data by adjusting the asymptotic mixing length corresponding to vanishing Richardson number. This data analysis and several studies from the literature have been used to construct a formulation for the Prandtl number. This Prandtl number is unity at neutral stratification and increases approximately linearly with increasing Richardson number for the range $0 \leqslant \mathrm{Ri} \leqslant 1$.

This formulation of local mixing is applied to a column model, sufficiently simple for use within large scale models. As an example, the model is applied to turbulence in the residual layer above the nocturnal surface inversion layer. During the night, weak turbulence develops at the top and bottom of the modeled residual layer due to shear associated with the low-level jet. Large scale subsidence can significantly reduce the thickness of the residual layer during the night.

In the upper part of the nocturnal surface inversion layer, the formulation for locally generated turbulent mixing *overrides* the surface-based boundary-layer formulation when boundary-layer similarity theory fails to represent the impact of the local shear on the underside of the nocturnal jet. With weak air flow in the very stable case, the local generation of turbulence at the top of the inversion layer may be the principal cause of diffusion corresponding to an *upside-down* boundary-layer structure. Such boundary layers belong to the Type I nocturnal boundary-layer class of Kurzeja et al. (1991). The turbulence generated at the top of the surface inversion layer leads to downward heat transport and warmer surface temperatures compared to the case where such local generation is not included.

Uncertainties in the mean subsidence and geostrophic wind prevent definitive testing of the mixing length formulations against observations. Without subsidence, the model fails to stratify the residual layer during the night. Omission of clear air radiative cooling, horizontal temperature advection, or underestimation of mixing probably contribute to underestimation of restratification of the residual layer. In future work, clear air radiative cooling will be included, which, unfortunately will reduce the model's current utility as an economic package for large scale models.

7. Acknowledgments

We gratefully acknowledge D. Lenschow for supplying the CABLE data and Markus Quante for providing flux values from ICE. The helpful comments of Anton Beljaar and the reviewers are appreciated. This material is based upon work supported by the Phillips Laboratory under contract F19628-88-K-0001 and the Physical Meteorology Program of the National Science Foundation under grant ATM-8912736.

REFERENCES

André, J. C., De Moore, G., Lacarrére, P., Therry, G. and Du Vachat, R. 1978. Modeling the 24 hr evolution of the mean and turbulent structures of the planetary boundary layer. *J. Atmos. Sci. 35*, 1861–1883.

André, J. C. and Mahrt, L. 1982. The nocturnal surface inversion and influence of clear-air radiative cooling. *J. Atmos. Sci. 39*, 864–878.

Atlas, D., Metcalf, J. I., Richter, J. H. and Gossard, E. E. 1970. The birth of "CAT" and microscale turbulence. *J. Atmos. Sci. 27*, 903–913.

Beljaars, A. C. M. and Holtslag, A. A. M. 1991. Flux parameterization over land surfaces for atmospheric models. *J. Appl. Meteor. 30*, 327–341.

Beyrich, F. and Klose, B. 1988. Some aspects of modeling low-level jets. *Bound.-Layer Meteor. 43*, 1–14.

Blackadar, A. K. 1962. The vertical distribution of wind and turbulent exchange in a neutral atmosphere. *J. Geophys. Res. 67*, 3095–3102.

Buajitti, K. and Blackadar, A. K. 1957. The theoretical studies of diurnal wind structure variation in the planetary boundary layer. *Quart. J. Roy. Meteorol. Soc. 83*, 486–500.

Busack, B. and Brümmer, B. 1988. A case study of Kelvin-Helmholtz waves within an off-shore stable boundary layer: Observations and linear model. *Bound.-Layer Meteor. 44*, 105–135.

DeSilva, I. P. D. and Fernando, H. J. S. 1992. The growth of a turbulent patch in a stratified fluid. To appear in *J. Fluid Mech. 00*, 000–000.

Dutton, J. A. 1969. An energy budget for a layer of stratospheric CAT. *Radio Sci. 4*, 1137–1142.

Ek, M. and Mahrt, L. 1990. *A user's guide to OSU1DPBL version 1.0.3: a one-dimensional planetary boundary layer model with interactive soil layers and plant canopy.* Department of Atmos. Sci., Oregon State University, Corvallis, OR 97331.

Estournel, C., Vehil, R. and Guedalia, D. 1986. An observational study of radiative and turbulent cooling in the nocturnal boundary layer (ECLATS EXPERIMENT). *Bound.-Layer Meteor. 34*, 55–62.

Fernando, H. J. S. 1991. Turbulent mixing in stratified fluids. *Ann. Rev. Fluid Mech. 23*, 455–493.

Garratt, J. R. and Brost, R. A. 1981. Radiative cooling effects within and above the nocturnal boundary layer. *J. Atmos. Sci. 38*, 2730–2746.

Garratt, J. R. 1985. The inland boundary layer at low altitudes. *Bound.-Layer Meteor. 42*, 307–327.

Heck, W. J., Panofsky, H. A. and Bender, M. A. 1977. The effect of clear-air turbulence on a model of the general circulation of the atmosphere. *Beiträge zur Physik der Atm. 50*, 89–97.

Hsu, S. A. 1979. Mesoscale nocturnal jetlike winds within the planetary boundary layer over a flat, open coast. *Bound.-Layer Meteor. 17*, 485–494.

Keller, J. L. 1990. Clear air turbulence as a response to meso- and synoptic-scale dynamic processes. *Mon. Wea. Rev. 118*, 2228–2242.

Kennedy, P. J. and Shapiro, M. A. 1975. The energy budget in a clear air turbulence zone as observed by aircraft. *Mon. Wea. Rev. 110*, 650–654.

Kennedy, P. J. and Shapiro, M. A. 1980. Further encounters with clear air turbulence in research aircraft. *J. Atmos. Sci. 37*, 986–993.

Kondo, J., Kanechika, O. and Yasuda, N. 1978. Heat and momentum transfer under strong stability in the atmospheric surface layer. *J. Atmos. Sci. 35*, 1012–1021.

Kunkel, K. E. and Walters, D. L. 1982. Intermittent turbulence measurements of the temperature structure parameter under very stable conditions. *Bound.-Layer Meteor. 22*, 49–60.

Kurzeja, R. J., Berman, S. and Weber, A. H. 1991. A climatological study of the nocturnal planetary boundary layer. *Bound.-Layer Meteor. 54*, 105–128.

Lenschow, D. H., Li, X. S., Zhu, C. J. and Stankov, B. B. 1987. The stably stratified boundary layer over the great plains. *Bound.-Layer Meteor. 42*, 95–121.

Louis, J. 1979. A parametric model of vertical eddy fluxes in the atmosphere. *Bound.-Layer Meteor. 17*, 187–202.

Louis, J., Tiedke, M. and Geleyn, J. F. 1981. A short history of the operational PBL parameterization at ECMWF. *Workshop on planetary boundary layer parameterization*, ECMWF, 59–79.

Lyons, R., Panofsky, H. A. and Wollaston, S. 1964. The critical Richardson number and its implications for forecast problems. *J. Appl. Meteorol. 21*, 136–142.

Mahrt, L. 1985a. Vertical structure and turbulence in the very stable boundary layer. *J. Atmos. Sci. 42*, 2333–2349.

Mahrt, L. 1985b. Turbulence in the coastal range over Northern Yugoslavia. *Zbornik Meteoroloskih Hydroloskih Radova 11*, 46–49.

Mahrt, L. and Gibson, W. 1992. Decomposition of fluxes into coherent structures. *Boundary-Layer Meteorol. 60*, in press.

Mahrt, L., Heald, R. C., Lenschow, D. H., Stankov, B. B.

and Troen, I. B. 1979. An observational study of the structure of the nocturnal boundary layer. *Bound.-Layer Meteor. 17*, 247–264.

Maryon, R. H. 1990. A statistical representation of sub-grid variation in mixing-length models of the turbulent boundary layer. *Bound.-Layer Meteor. 53*, 371–399.

Merrit, G. and Rudinger, G. 1973. Thermal and momentum diffusivity measurements in a turbulent stratified flow. *AIAA J. 11*, 1465–1470.

Mizushina, T., Ogino, F., Ueda, H. and Komori, S. 1978. Buoyancy effects on eddy diffusivities in thermally stratified flow in an open channel. *Heat transfer 1978, 1*, 91–96, New York, Hemisphere Publishing Co.

Nappo, C. J. 1991. Sporadic breakdowns of stability in the PBL over simple and complex terrain. *Bound.-Layer Meteor. 54*, 69–87.

Nieuwstadt, F. T. M. 1984. The turbulent structure of the stable, nocturnal boundary layer. *J. Atmos. Sci. 41*, 2202–2216.

NMC Development Division Staff. 1988. Documentation of the research version of the Medium Range Forecast model. *NMC Documentation Series #1*. Development Division, NMC, Washington DC, 20233.

Padman, L. and Jones, I. S. F. 1985. Richardson number statistics in the seasonal thermocline. *J. Phys. Oceanogr. 15(7)*, 844–854.

Quante, Markus. 1989. *Flugzeug Messungen der Turbulenzstruktur in Cirruswolken.* Institut für Geophysik und Meteorologie, Heft 65, Universität zu Köln.

Roach, W. T. 1970. On the influence of synoptic development on the production of high level turbulence. *Quart. J. Roy. Meteorol. Soc. 96*, 413–429.

Rohr, J. J., Itsweire, E. C., Helland, K. N. and Van Atta, C. W. 1988. Growth and decay of turbulence in a stably stratified shear flow. *J. Fluid Mech. 187*, 1–34.

Ruscher, P. H. 1987. *An examination of structure and parameterization of turbulence in the stably-stratified atmospheric boundary layer.* Ph.D. thesis, Oregon State University. 170 pp.

Smith, B. and Mahrt, L. 1981. A study of boundary layer adjustments. *J. Atmos. Sci. 38*, 334–346.

Stull, R. B. and Driedonks, A. G. M. 1987. Applications of the transilient turbulence parameterization to atmospheric boundary layer simulations. *Bound.-Layer Meteor. 40*, 209–239.

Stull, R. B. 1990. *An introduction to boundary layer meteorology.* Boston, Kluwer Academic Publishers. 666 pp.

Thorpe, S. A. 1973. Turbulence in stably stratified fluids: A review of laboratory experiments. *Bound.-Layer Meteor. 5*, 95–119.

Troen, I. B. and Mahrt, L. 1986. A simple model of the atmospheric boundary layers; sensitivity to surface evaporation. *Bound.-Layer Meteor. 37*, 129–148.

Ueda, H., Mitsumoto, S. and Komori, S. 1981. Buoyancy effects on the turbulent transport processes in the lower atmosphere. *Quart. J. Roy. Meteorol. Soc. 107*, 561–578.

Vinnichenko, N. K., Pinus, N. Z., Stameter, S. M. and Shur, G. N. 1973. Turbulence in the free atmosphere. John Dutton, Translation editor, Consultants Bureau. New York. 263 pp.

Webster, C. A. G. 1964. An experimental study of turbulence in a density-stratified shear flow. *Fluid Mech. 19*, 221–245.

Wittich, K.-P. and Roth, R. 1984. A case study of nocturnal wind and temperature profiles over the inhomogeneous terrain of Northern Germany with some considerations of turbulent fluxes. *Bound.-Layer Meteor. 28*, 169–186.

Wu, S. S. 1965. A study of heat transfer coefficients in the lowest 400 meters of the atmosphere. *J. Geophys. Res. 70*, 1801–1807.

Yasuda, N. 1988. Turbulent diffusivity and diurnal variations in the atmospheric boundary layer. *Bound.-Layer Meteor. 43*, 209–222.